518 *Macromolecules* **2010**, *43*, 518–524
DOI: 10.1021/ma9017185

Macromolecules
ARTICLE

Molecular Observation of Branch Point Motion in Star Polymer Melts

Michaela Zamponi,*,† Wim Pyckhout-Hintzen,† Andreas Wischnewski,† Michael Monkenbusch,† Lutz Willner,† György Kali,‡ and Dieter Richter†

†*Forschungszentrum Jülich, 52425 Jülich, Germany and* ‡*Institut Laue-Langevin, 6 rue Jules Horowitz, 38000 Grenoble, France*

Received August 1, 2009; Revised Manuscript Received October 30, 2009

ABSTRACT: Using neutron spin echo (NSE) spectroscopy and a labeling scheme unique to neutron scattering the motion of a labeled branch point of a three-arm polyethylene star has been observed on a molecular level. The measured dynamic structure factor shows a clear transition to a plateau, signifying the stronger confinement of the star center in comparison to a corresponding center labeled linear chain. A shortening of one star arm to about only one entanglement length leads to the same topological confinement as for the symmetric star within the accessible time range of NSE. This reflects a stronger effect of such a small branch than expected and is consistent with rheological measurements on the same system.

I. Introduction

The dynamics of polymer melts not only depends on the chain length but even more so on the polymer architecture. By introducing a branching point the chain dynamics is considerably slowed down. In order to describe the elastic response of branched polymers (stars, H-polymers, ...) in rheological measurements a hierarchical relaxation has been postulated.[1] Similar as for linear chains the confinement of branched polymers can be described by a tube model, where each branch is confined in a tube. However, unlike linear chains, the polymer can not reptate; the branch point localizes the polymer in space until the different arms have fully relaxed to the branch point. Deeper arm retractions are facing an entropic barrier leading to long time scales that exponentially depend on the branch length. Therefore, arm retraction and branch point motion are well separated, which is signified in the dynamic modulus by a broad relaxation spectrum. In order to describe the dynamic modulus quantitatively the full spectrum of time scales has to be considered. Milner and McLeish[2] successfully described the dynamics for symmetric stars by including the effect of dynamic tube dilution caused by the already relaxed chain segments. Frischknecht et al.[3] extended the theory to the case of asymmetric stars by considering that the short arm relaxes much faster than the longer arms and eventually allows the star to reptate. They found, however, that the drag of a short arm of only a few entanglements in asymmetric stars imposes a larger drag than expected.

The combination of neutron spin echo spectroscopy and a labeling scheme unique to neutron scattering allowed now for the first time the direct observation of the branch point motion on a molecular level. We report on NSE measurements on two different three-arm stars: one symmetric star with long well entangled star arms and one asymmetric star where the third arm was shortened to a length of only one entanglement length. In both cases, only the nearest segments around the branch point have been labeled (protonated in an otherwise deuterated melt) and hence allow the observation of the branch point motion. The stars have been compared to a corresponding center labeled linear chain. For both stars a strong localization of the branch point has been observed, whereas the center of the linear chain displays diffusive motion of the chain along the tube. Surprisingly within the observation window the short arm of only one entanglement length already leads to the same confinement as for the much longer star arm. The accessible time range by NSE is restricted to a few 100 ns by its resolution limit. In order to observe the full relaxation spectrum, rheological measurements on the same system have been performed. The rheological findings agree with the neutron scattering results and can be well described by Frischknecht's ansatz. Again the drag caused by the short arm is found to be stronger than expected. A recent molecular dynamics (MD) simulation by Zhou and Larson[4] on asymmetric stars also gave the indication of a stronger slowing down due to short side arms. But they also showed that after the short arm retraction time the branch point performs a distinctive hopping motion. Comparison of the time scales with our system suggests that the hopping would be within the accessible NSE time range but the experimental data give no indication of that.

The paper is organized as follows: in section II a brief summary of the theory is given, and in section III the experimental details are described. The results are then presented and analyzed in section IV. The comparison between the different methods is discussed in section V, and in section VI the results are summarized.

II. Theory

A. Hierarchical Relaxation. The tube model by Edwards[5] and DeGennes[6] successfully describes the dynamics in well entangled linear polymer melts. The chains are confined laterally inside the tube and perform a one-dimensional Rouse motion along the tube and a slow diffusion creep motion out of the tube. With decreasing chain length reptation limiting processes such as contour length fluctuations (CLF) and constraint release (CR) become important. In the linear case these processes compete with the reptation motion at longer times but for branched systems these processes are the crucial relaxation mechanisms. The branch point localizes the polymer so that it cannot reptate. Hence, in star polymers the arms have to fully retract to the branch point within one entanglement length before the whole star can move.

*Corresonding author. E-mail: m.zamponi@fz-juelich.de.

 Published on Web 11/20/2009

Deeper arm retractions are exponentially slowed down with the arm length since they are entropically not favorable. This leads to a broad spectrum of relaxation times in the dynamic modulus. Constraint release of the star arms in addition causes dynamic tube dilution effects. For highly asymmetric stars the relaxation times of the short arm is much smaller than the relaxation times of the longer arms. Therefore, when the short arm has fully retracted the longer arms are still well entangled. However, the short arm can then be dragged into the tube of the long arms, so that the star can diffuse along the tube contour as a linear chain albeit with a larger drag due to the short arm. After the short arm retraction time τ_s^* when the short arm has retracted fully to the branch point, the branch point is expected to perform a diffusive hop motion with jumps in the order of the tube diameter d. The diffusion constant of the branch point is then $D_{hop} = p^2d^2/(2\tau_s^*)$ where p is a dimensionless constant to allow hopping of a fraction of the tube diameter. This parameter p is expected to be close to unity but for short arms of only a few entanglements Frischknecht et al.[3] found this value for asymmetric stars to be much smaller than 1. Similar results were found in recent MD simulations by Zhou et al.[4]

B. Modeling of G*(ω). For the description of the dynamic moduli we follow closely the work of Frischknecht et al.[3] for the branched polymers. For the linear reference polymer the Likhtman−McLeish model[7] was used, which allows to extract basic parameters like plateau modulus G_e and the entanglement time τ_e as well as the constraint release parameter c_v. Theses models are described very well in the literature and will not be repeated in detail here. Instead a rough outline is given: rapid Rouse motion inside a tube for times smaller than the entanglement time τ_e are followed by an activated process of entropy-controlled fluctuations toward the branching point in a more or less widening tube due to relaxing chain ends. This problem of different time scales of motions along arms of a chain which are tethered in a branching point, give the need to estimate the full hierarchical time scale spectrum as well as the reduction of the entanglement density. This is generalized as

$$G(t) = \int_0^1 \frac{\partial G(\Phi(s))}{\partial s} \exp(-t/\tau(s))\, \mathrm{d}s \qquad (1)$$

where $\Phi(s)$ is the tube occupation factor of segments with s the fractional distance along the arms and $\tau(s)$ is the spectrum of relaxation times. The integral runs over all coordinates of the arms. $G(t)$ is the stress relaxation modulus which is related to the complex modulus $G^*(\omega)$ by Fourier transformation.

For early times the effective potential barrier U_{eff} is negligible, the chain ends diffuse by Rouse motion inside the tube. The time scale for this process is

$$\tau_{early} = \frac{225\pi^3}{256}\tau_e\left(\frac{N}{N_e}\right)^4 s^4 \qquad (2)$$

with N_e the length of an entanglement strand.[2] In literature also a smaller prefactor for τ_{early} is used,[8] stemming from the use of different definitions for $G_e(M_e)$ which also influence the full relaxation time. For deeper arm retractions the chain ends have to overcome the potential barrier, the process is activated. In the asymmetric case, it is further taken into account that after the time $\tau_s^* = \tau_s(s_s = 1)$ when the short arm is relaxed fully, only a certain fraction s_l of the long arms has lost its tube. This has consequences for the amount of dynamic dilution present. The latter appears in the exponent Φ^α with $\alpha = {}^4/_3$ that is kept fixed in the calculations. The time scale for the activated process τ_{late} is calculated for the short arm and for the long arm before and after the short arm retraction time.[3] In order to calculate the full arm retraction times a crossover function is used:[9]

$$\tau_a(s) = \frac{\tau_{early}(s)\exp(U_{eff}(s))}{1+\exp(U_{eff}(s))\tau_{early}(s)/\tau_{late}(s)} \qquad (3)$$

After the short arm has fully relaxed the asymmetric star (unlike the symmetric star) eventually can reptate along the remaining tube of the long arms. The short arm imposes an extra drag on the diffusive motion of the chain. The retracted arm together with its branch point can then hop by a maximal distance of the tube diameter. Then the effective diffusion can be calculated by $1/D_{\mathrm{eff}} = 1/D_R + 1/D_{hop}$. $D_R = k_{\mathrm{B}}T/(2N_l\xi)$ is the Rouse diffusion constant of the backbone with N_l the number of segments of the long arm and ξ the segmental friction. With the effective diffusion constant the reptation time for the backbone can be calculated. In our case the fraction of short arms is so small that dilution effects can be neglected and we assume hopping and reptation in the undiluted ("skinny") tube. The reptation regime starts, when the relaxation via reptation is faster than the arm retraction, i.e. when the long arm retraction time equals the reptation time of the backbone: $\tau_l(s_d) = \tau_d$. The reptation time without dilution effects is then[3]

$$\tau_d = \frac{15}{4}\left(\frac{2N_l}{N_e}\right)^3 \tau_e(1-s_d)^2\left(1+\frac{5}{6\pi^2p^2 2N_l/N_e}\frac{\tau_s^*}{\tau_e}\right) \qquad (4)$$

C. Dynamic Structure Factor. The use of neutron scattering allows to access the dynamics on a molecular level. Because of contrasting by specific labeling with protons or deuterons it is possible to measure the pair correlation function of segments along the chain, the coherent dynamic structure factor $S(q,t)$. For linear polymers, analytical descriptions of the dynamic structure factor exist. Dependent on the chain length different models are able to describe the dynamic behavior. The dynamics of short unentangled chains is determined by a balance of viscous and entropic forces which is described in the Rouse model by a chain in a heat bath.[10] With the calculated Rouse modes the dynamic structure factor can be calculated as the correlation function of the chain segments

$$S(q,t) = \sum_n \sum_m \exp\left(-\frac{q^2}{6}\langle(R(m,t)-R(n,0))^2\rangle\right) \qquad (5)$$

where the sums run over all segments n, m and q is the momentum transfer.

For longer chains entanglement effects come into play, the chains mutually restrict each other in their motion. Only until the entanglement time τ_e the chains can perform free Rouse motion. Then they start to feel their mutually restriction. This can be described by a virtual tube which confines the motion to a local reptation inside the tube and a slow diffusive creep motion out of the tube. DeGennes calculated the dynamic structure factor as[11]

$$S(q,t)/S(q) = (1-F(q))S_{loc}(q,t/\tau_0) + F(q)S_{creep}(q,t/\tau_d) \qquad (6)$$

with $F(q) = \exp(-(qd/6)^2)$ the tube form factor, while the time scale is $\tau_0 = 36/(Wl^4q^4)$ and the disentanglement time is $\tau_d = 3N^3l^2/(\pi^2d^2W)$. This form has been corroborated for long polymers by neutron spin echo spectroscopy.[12] However, comparison of other predictions of the reptation model with experimental findings as, e.g., the molecular weight dependence of the viscosity already gave the indication early on that other additional relaxation processes must exist.[13] The original tube model assumes that the only process which releases the constraints is the reptation motion of the confined chain out of the initial tube. However, fluctuations of the chain ends and motions of the chains building the tube also cause loss of confinement. Recently it has been proven on a molecular level that contour length fluctuations[14] and constraint release[15] contribute to the faster relaxation for chains of intermediate lengths. CLF is an effect of the chain ends, by masking them out the center segments display the full tube constraints as a very long chain.[16]

For the case of a short label in the middle of the chain a neutron scattering experiment at low enough q observes the self-motion of this label. Thus, under these circumstances we would see the segmental motion along the tube. In our experiment the label size of $\langle R_g^2\rangle_{label}^{1/2} = 20$ Å is in between the situation of collective dynamics seen for a fully labeled chain and that of a labeled segment. For this finite label size an analytical scattering function is not available. Nevertheless, with increasing segmental mean square displacement, we expect a gradual transition from the collective chain structure factor to that for the self-motion.

To describe the branch point confinement we follow the theory of Vilgis and Boué[17] which describes the constraints imposed by permanent cross-links in a network on the chain segments. On the basis of the Rouse dynamics they model the effect of the cross-links by introducing a common harmonic potential for all segments. The mean square displacement for those confined segments can then be calculated as

$$\langle (R(m,t)-R(n,0))^2\rangle = 3R_m{}^2\left[1-\frac{1}{2}\left(2\cosh\left(\frac{l^2}{3R_m{}^2}|n-m|\right)\right.\right.$$
$$-\exp\left(-|n-m|\frac{l^2}{3R_m{}^2}\right)\operatorname{erf}\left(\frac{1}{3R_m{}^2}\sqrt{Wl^4t}-|n-m|\frac{l^2}{2\sqrt{Wl^4t}}\right)$$
$$\left.\left.-\exp\left(|n-m|\frac{l^2}{3R_m{}^2}\right)\operatorname{erf}\left(\frac{1}{3R_m{}^2}\sqrt{Wl^4t}+|n-m|\frac{l^2}{2\sqrt{Wl^4t}}\right)\right)\right] \quad (7)$$

with n, m segments number, l the segment length, Wl^4 the Rouse rate, and R_m the well parameter which corresponds to the radius of gyration of the mesh. The only unknown parameter is the well parameter, which gives the size of the confinement: $R_m{}^2 = 1/6N_el^2 = 1/6d^{*2}$ The other parameters can be obtained from measurements on linear chains. As was shown by Warner,[18] for branched systems the friction at the branch point is stronger, resulting in a reduced Rouse rate: $W^* = 2/fW$ with f the functionality of the branch point (here $f = 3$). With the availability of the mean square displacement the dynamic structure factor can then be easily calculated according eq 5.

III. Experimental Section

A. Sample Preparation. The partly labeled linear and branched polyethylenes (PE) have been synthesized by anionic polymerization of polybutadiene (PB) with subsequent deuteration. The symmetric star consists of 3 arms with a length of about 26 kg/mol each, where only about 1 kg/mol at the junction of the arms were protonated, the rest of the arms deuterated and hence not visible in the neutron scattering experiments. The length of the short arm of the asymmetric star is about only one entanglement length (~2 kg/mol) but the label of the branch point is as before. The length and label of the linear chain correspond to the two long arms with the protonated part in the center (see schematic view Figure 1).

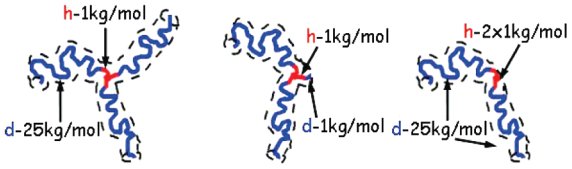

Figure 1. Schematic drawing of the synthesized polymers with nominal molecular weights.

The linear triblockcopolymer and the blockcopolymers for the different star arms have been prepared by sequential addition of *H*- or *D*-butadiene under high vacuum conditions. The reaction time for each block was about 2 days to ensure a completed polymerization for each block. For the linear triblockcopolymer the living chains have been terminated by methanol. For the branched polymers the coupling agent trichlormethylsilane was added to the living arms. For the symmetric star only about 30% of the stoichiometric quantity was added in order to avoid a contamination with not fully coupled stars ("two-arm stars"). The remaining linear chains have been terminated with methanol prior to opening the reactor. By fractionation in a solution of toluene and methanol the linear chains have been removed. In the case of the asymmetric star the short arm was first mixed with an excess of the coupling agent to minimize multiple substitution. After removing the remaining coupling agent a slight excess of the living long arms were added. By fractionation of the finalized stars the terminated linear chains and asymmetric stars with two short arms have been separated.

The characterization of the blocks has been performed after each step on the PB parent polymers by size exclusion chromatography (SEC). Since the block molecular weights are determined as a difference of two SEC measurements these values have a larger error and the sum differs slightly from the total molecular weight (see Table 1).

The parent polybutadienes have been used for the rheological measurements since polyethylene crystallizes and hence limit the accessible time−temperature range. For the neutron spin echo background measurements a fully deuterated symmetric star of comparable molecular weight has been synthesized for the branched systems (which was also used for the rheological measurement, $M_w^{arm} = 28.8$ kg/mol) and as background for the linear polymer a fully deuterated linear chain sample has been used. For the NSE measurements the polymers have been saturated with deuterium under pressure at 373K with Palladium on Bariumsulfat as catalyst in order to obtain the temperature stable polyethylenes (PEB-2). The finished samples have been filled in standard niobium container under inert atmosphere and sealed with Teflon.

B. Neutron Scattering. Neutron spin echo spectroscopy[19] measures directly the intermediate scattering function $S(q,t)/S(q)$. The momentum transfer q in the quasi-elastic case relates to the wavelength λ as $q = (4\pi/\lambda)\sin(\theta/2)$ with θ being the scattering angle. Protons and deuterons have different neutron scattering lengths. For few protonated or partly labeled chains in a deuterated matrix the coherent dynamic structure factor is measured which reveals the effect of segment−segment pair correlations within the labeled section of one polymer. For fully protonated samples or randomly labeled chains the incoherent dynamic structure factor is observed which yields the segment

Table 1. Molecular Characteristics of the Parent Polybutadiene Polymers

	M_w^{ges} [kg/mol][a]	M_w/M_n[b]	M_w^{block} [kg/mol][c]
linear chain	58.3	1.04	d26.4−h3.5−d26.2
symmetric star	74.3	1.04	d25.8−h1.05
asymmetric star	55.7	1.03	d/h28.6−d/h2.1

[a] Molecular weight of complete polymer determined by light scattering. [b] Polydispersity, SEC conventional calibration. [c] Molecular weights of the different blocks: linear chain, SEC conventional calibration; symmetric star, SEC light scattering-SEC ^{1}H-NMR, weights for each arm; asymmetric star, SEC conventional calibration-SEC universal calibration, total weight for the different arm lengths with nominal label d25-h1 and d1-h1 respectively.

self-correlation, in the first case in form of the spin-incoherent scattering of the protons in the latter case as a kind of isotope incoherent scattering on the scale of the segments. In our case, for the partly labeled linear chain, the label size is so small that in the small angle scattering regime of NSE we observe only a small contribution of the correlated scattering of the chain segments but mainly the self-correlation of the labeled section as a whole.

The measurements were performed at the IN15 at the Institut Laue-Langevin at a temperature of 509 K and a wavelength of about 15 Å, covering a q-range of 0.03 to 0.115 Å^{-1}. The data were corrected for resolution and background; the latter was obtained from the fully deuterated samples.

C. Rheology. The linear viscoelastic properties of the parent polybutadiene (PB) star and the linear PB polymers, prior to hydrogenation which led to the PE counterparts, were measured at an ARES Rheometer (Rheometrics Sci) using a 2K FRNT transducer in oscillatory shear and in the parallel plate geometry with a diameter of 25 mm. Isothermal temperature sweeps between −65 and +40 °C in steps of 15 °C under a nitrogen gas blanket were performed on previously vacuum-molded samples of about 1.3 mm thickness, thereby varying the frequency ω between 10^{-2} and 10^2 rad/s. The strain amplitude was kept in the range 1−2% to ensure linearity over the full range. 6−8 points per decade in frequency were measured. Horizontal and vertical shift factors were obtained from a two-dimensional shifting. To exclude artifacts simultaneous shifting was compared to consecutive frequency and amplitude correction. Compatible curves were obtained. Average C_1 and C_2 factors were determined from fitting the WLF equation $\log a_T = -C_1(T - T_0)/(C_2 + (T - T_0))$ to the temperature dependent shift factors a_T. The chosen reference temperature is $T_0 = 25$ °C. The vertical shift factors between 0.98 and 1.09 were roughly comparable to the expected ratio of $(\rho T/\rho_0 T_0)$ using literature values. Consistency between the different experiments is evident from the good overlap for the linear and the different branched architectures in the Rouse regime. The WLF parameters that were separately determined for each architecture were identical within 1 standard deviation.

IV. Results and Analysis

A. NSE. In order to investigate the stronger confinement in branched polymer systems, neutron spin echo spectroscopy has been performed on a symmetric three-arm star where only the branch point was labeled. Keeping the label of the branch point as before, the length of one of the star arms was shortened to about only one entanglement and further to a linear "two-arm star" to study the influence of the third arm on the branch point motion.

In Figure 2 the dynamic structure factor for different q of the branch point labeled symmetric star is shown and compared to the linear reference sample. For better visibility not all measured q-values are shown. For about the first 35 ns, star and linear chain display the same relaxation, but then the structure factor of the star levels off into a plateau region whereas the structure factor of the center labeled

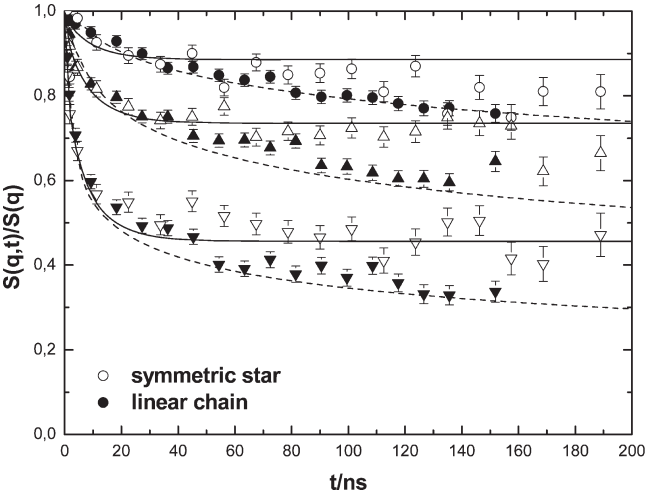

Figure 2. Dynamic structure factor of a center labeled linear chain (closed symbols) in comparison to a branch point labeled symmetric three-arm star (open symbols). Q-values (in Å^{-1}): 0.05 (circles), 0.077 (triangles up), 0.115 (triangles down). Dashed lines are guides for the eye; solid lines fit with eq 5.

linear chain continues to decay. The plateau in the dynamic structure factor signifies the extra confinement of the branch point motion. The segmental mean square displacement at the transition time into the plateau regime is $\langle r^2(t)\rangle^{1/2} = (4Wl^4t/\pi)^{1/4} = 42$ Å (using the value of $Wl^4 = 70000$ Å^4/ns of the linear chain),[20] providing an estimate for the localization space of the branch point.

Although the center of the linear chain is also still well confined inside a tube built by the surrounding chains, the segments may move freely along the tube, causing the additional relaxation of the dynamic structure factor. At the time of the plateau formation in the branch point structure factor, the segments of the linear chain have already moved further than the extension of the label. For a small enough label size and at small enough q, the fluctuations within the label do not further contribute to the decay of $S(q,t)$ but the motion of the labeled chain section itself is observed; i.e., we observe the self-motion of the label. Thus, the experiment visualizes the local reptation dynamics, where the chain segments undergo Rouse motion along the tube and the mean square displacement is expected to increase with a $t^{1/4}$ power law. Plotting the data displayed in Figure 2 in the form $\log(-(6/q^2)\ln(S(q,t)/S(q)))$ vs $\log(t)$ (see Figure 3), the asymptotic emergence of this power law may be directly seen. Thus, the scattering function measured from the center labeled linear chain transforms gradually in character from a pair correlation function at short times to a self-correlation function at long times.

Since there exist no theoretical descriptions for this gradual crossover, we now scrutinize the data with expressions available for the two limits and also relate to previously published data for chains featuring a long center label[16] where the above effect should not appear. Thus, in Figure 4 we compare (i) the reptation prediction for the single chain dynamic structure factor, valid for a long labeled chain, (ii) experimental results for a chain with a long label in the center that masks contour length fluctuations and visualizes the full tube constraints, (iii) our new results with the short label in the center and (iv) the prediction of Fatkullin and Kimmich[21] for self-motion. While $S(q,t)$ from the chain with the long label agrees well with the predicted single chain dynamic structure factor for reptation, as discussed above at longer times the data from

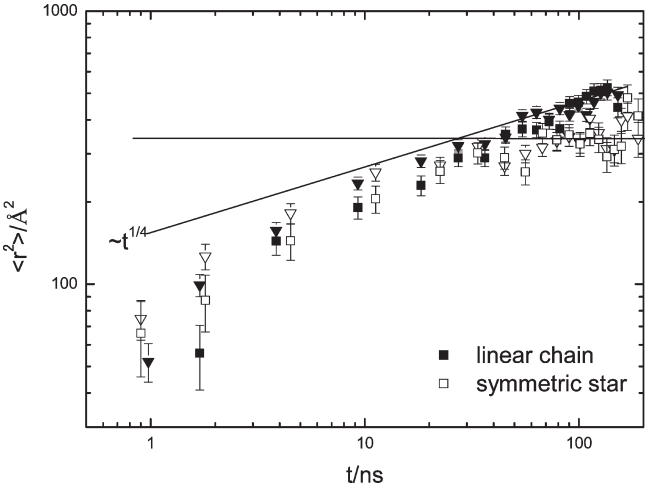

Figure 3. Asymptotic effective mean square displacement (MSD) as obtained from the dynamic structure factor from the center labeled linear chain (closed symbols) for 2 q values (0.077 Å^{-1} (squares), 0.115 Å^{-1} (triangles)). For long times the $t^{1/4}$ of local reptation is approached. For comparison the corresponding data from the branch point labeled star are included (open symbols) displaying a plateau at long times.

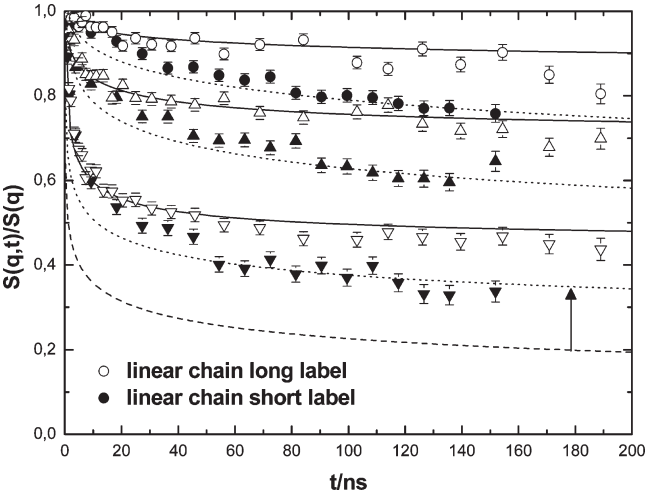

Figure 4. Illustration of the finite label size effect: dynamic structure factor of a linear chain with finite center label (3.5 kg/mol label in 58 kg/mol chain, closed symbols) in comparison to the expectation of the reptation model (eq 6, solid lines) and a linear chain with long center label (20 kg/mol label in 28 kg/mol chain,[16] open symbols). The dashed line is the prediction of Fatkullin and Kimmich[21] for the highest q-value, dotted lines shifted $S(q,t)_{FK}$. Q values (in Å^{-1}): 0.05 (circles), 0.077 (triangles up), and 0.115 (triangles down).

the chain with the short label further decay and feature the gradual transition from collective to self-motion. Fatkullin and Kimmich have calculated the dynamic structure factor for self-motion along the tube $S(q,t)_{FK}$ considering important non Gaussianity effects.[21] In Figure 4, their prediction is shown as a dashed line for the highest q. As for the self-motion in the case of the Rouse dynamics their structure factor decays overall more strongly than that for the single chain. Nevertheless, the line shape at longer times is very accurately predicted, as shown by a shift of $S(q,t)_{FK}$ upward through the data (dotted lines). We hypothesize that the necessary shift relates to coherency effects at short times.

In order for the branch point to be able to move in the accessible time window, the third arm has been reduced to only one entanglement length. Then the short arm should not be entangled and should be able to move along the tube of the two long arms, causing only a stronger friction. Even considering the entropic barrier imposed by the branch point the short arm would be expected to relax within the NSE time range and enable the diffusive motion of the branch point. In Figure 5, the measured dynamic structure factor of the branch point labeled asymmetric star in comparison to the corresponding symmetric three-arm star is shown. Surprisingly, within the errors no difference can be observed, both structure factors transit into a plateau region, signifying the constraints of the branching point. Although the length of the third star arm amounts to just about one M_e obviously this very short arm length is already sufficient to localize the branch point as in the case of the much longer arm. We thus conclude that the relaxation time of the short arm is larger than the maximum NSE observation time $\tau_s^* > 190$ ns.

To quantify the effect of the branch point confinement we applied the theory of Vilgis and Boué[17] that describes the dynamic of confined chain segments in a harmonic potential of a size defining the effective confinement. The summations in eq 5 are done only for the labeled segments, assuming the labeling scheme as in the linear case. The segment length is known for linear PE (4.12 Å) as well as the segmental friction or Rouse rate $Wl^4 = 70000$ Å^4/ns.[20] For the branch point the Rouse rate is expected to be reduced by a factor 2/3.[18] The only unknown parameter is the confinement size of the branch point. The dashed lines in Figure 5 show the fit with

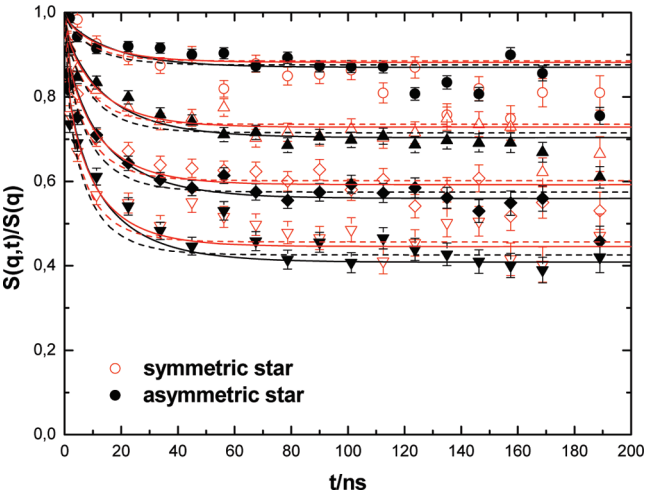

Figure 5. Dynamic structure factor of a branch point labeled asymmetric three-arm star (closed symbols) in comparison to a branch point labeled symmetric three-arm star (open symbols). Q values (in Å^{-1}): 0.05 (circles), 0.077 (triangles up), 0.096 (diamonds), and 0.115 (triangles down). Lines fit with eq 5, dashed: well parameter only free parameter, solid: segmental friction additional free parameter.

the model of Vilgis and Boué, resulting in $d^* = 38$ Å for the symmetric and $d^* = 39$ Å for the asymmetric star. The fits can be slightly improved by additional fitting the friction (Figure 5, solid lines) resulting in a Rouse rate of about 33000 and 30000 Å^4/ns, respectively, and a bit larger confinement size of $d^* = 39$ and 40 Å, respectively. Thus, the confinement of the branch point is stronger than the tube confinement for the linear case where the tube diameter is $d^* = 47$ Å.[14] The fitted Rouse rate implies a friction that is a factor 1.5 larger than the anticipated value at the branch point and more than a factor 2 than the bulk value. Apparently the vicinity of the branch point at least up to the extent of the label size is affected by this type of retardation.

B. Rheology. Rheological measurements have been performed on the parent polybutadienes (PB) (Figure 6). Very

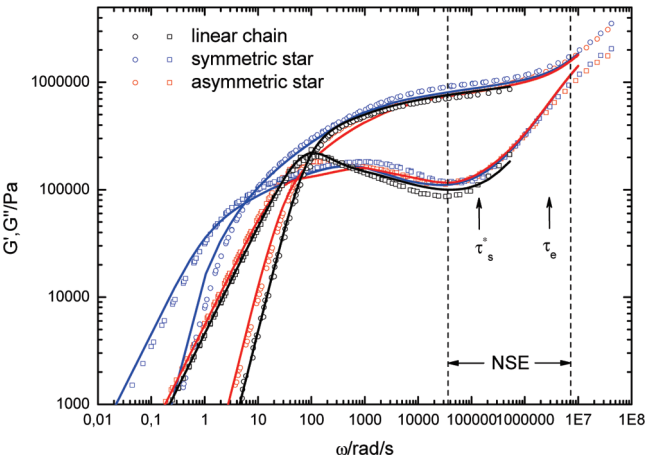

Figure 6. Loss (squares) and storage (circles) modulus of the parent polybutadienes at the reference temperature of 25 °C. Solid lines see text. Dashed lines indicate the corresponding accessible NSE time range and the arrows the time scales for PB at room temperature.

similar information on the branched structure or its influence should be expected, especially due to the very similar entanglement distance between PE and PB. Whereas M_e is about 1900 g/mol for PB at room temperature, the corresponding mesh size of the entangled PE as determined by rheological measurement is approximately 1200 g/mol (at $T = 413$ K).[22] Small deviations could reveal themselves if our experiments would be sensitive already in the limit of roughly 0.5−1 entanglements. The shortest arm in the case of PB is just over $Z = 1$, Z being the number of entanglements whereas it may be already 1.5 in the PE-case. We note, however, that the entanglement molecular weight obtained from NSE measurements of the tube diameter ($M_e = 1900$ g/mol for PE at 509K) is larger than deducted from rheological measurements. This systematic discrepancy of the confinement size as determined from NSE and rheology was also found for other polymers (PEP, PEO).[23,24]

Rheological measurements allow to observe the imprint of the molecular polymer dynamics on the polymer flow behavior covering thereby the whole time range of interest. At high frequencies the Rouse modes are accessed. As expected in the Rouse regime all three polymers show the same behavior. At intermediate times the loss modulus G'' of the linear chain follows a power law of about $-1/4$ due to CLF and CR until the transition into the reptation peak, whereas both star polymers display the characteristic spectrum of branched systems. In this intermediate time regime, the dynamic modulus of the asymmetric star is very much alike that of the symmetric star, only around the terminal time of the linear chain τ_d the asymmetric star displays a behavior similar to the linear chain; it flows, whereas the symmetric star needs more time to disentangle.

For a quantitative description of the dynamic moduli the theories of Likhtman[7] for the linear chain and Frischknecht[3] for the stars as described in section II were used. In the case of the linear chain G_e, τ_e, Z and the constraint release parameter c_ν were fitted, resulting in $G_e = 1$ MPa, $\tau_e = 0.35 \times 10^{-6}$ s, $Z = 29$, and $c_\nu = 0.06$. A value of $c_\nu = 0$ would mean no constraint release; a value of $c_\nu = 1$ would correspond to full CR contribution.[7] The fitted plateau modulus is close to the expected value of 1.15 MPa.[22] The entanglement molecular weight determined from Z is 1900 g/mol, well in agreement with the literature value of 1930 g/mol,[22] whereas M_e calculated from G_e is 2200 g/mol. Even larger deviations when both parameter were fitted independently have been reported.[7,8]

To scrutinize the data the Fourier transformation for the branched model was performed numerically in MAPLE and compared to the experimental data in order to obtain Z, G_e, and τ_e. The width of the dynamic moduli in time is strongly dependent on the actual number of Z, the amplitude is less severely affected by Z, and the entanglement time τ_e is a characteristic for the polymer and depends on the monomeric friction coefficient and the tube diameter. The fitted plateau modulus from the linear chain was also used for the branched systems. The fitted number of entanglements in all cases gives a M_e close to the expected value of 1900 kg/mol. In order to describe the Rouse regime of the branched polymers a slightly smaller entanglement time of $\tau_e = 0.2 \times 10^{-6}$s was needed. If we apply the Frischknecht theory to the linear polymer, then we get the same smaller τ_e, but the theory does not describe the data very well. There might be a small internal inconsistency between these two theories. The hopping was assumed to take place in a "skinny" tube, since dilution effects of the small arm are negligible. In order to be able to describe the asymmetric data, the "hopping fraction" was set to 1/60 following Frischknechts observation that this value for asymmetric stars with short arms is very low. Calculating the model with a value of $p^2 = 1$ leads to a spectral width which is about a decade too small. Frischknecht et al. investigated asymmetric PI stars with short arms down to $2.5M_e$, where a strong variation of p^2 with the arm length was needed, in order to be able to describe the data.[3] Decreasing p^2 results in a broadening of the spectrum and a softening of the reptation peak.

The agreement of the three different data sets with their corresponding theories is good (see Figure 6). In the linear case, small deviations are visible in the transition region between Rouse and CLF regime which might be improved by changing c_ν. For the symmetric star, the intermediate frequency regime shows some deviations. For the asymmetric star, the reptation peak is underestimated. This might be an indication that the limit of the linear case is not well described in Frischknecht's theory. Asymmetric stars with a side arm of a few entanglements are well described with the model.[3] But applying this theory directly to the linear data gives only a poor description of the loss and storage modulus. Therefore, the quantitative value for the arm relaxation time of only one entanglement might not be accurate. The reptation time of the linear chain with the correction of CLF is 0.013 s whereas the reptation time of the backbone of the asymmetric star is 0.029 s.

V. Discussion

A. Comparison NSE/Rheology. The rheological results agree largely with the NSE findings: the fitted entanglement time for PB at room temperature is $\tau_e = 0.35 \times 10^{-6}$s.With the determined shift factor for the linear chain of $a_T = 1.34 \times 10^{-2}$ this would give τ_e(509K, PB) = 5 ns which is comparable to τ_e(509 K, PE) = 7 ns. If we take the longest NSE time of about 200 ns and use the average shift factor, this time would translate to about 4×10^4 rad/s as indicated in Figure 6. In this accessible NSE time range G'' of the asymmetric star agrees with the symmetric star. Only at longer times (lower frequencies) the difference in the third star arm length comes into play: the asymmetric star displays a flow behavior similar to the linear chain.

Although the short arm in the asymmetric case has a length of only about one entanglement, with both experimental methods hardly any difference between the two branched polymers is visible in the intermediate time range. For the case of a linear chain of about

2 kg/mol the chain ends would be released via contour length fluctuations after a few nanoseconds ($s = 1$)[7] $\tau_{CLF}(s) = \tau_e(N/N_e)^4(2/1.5)^4 s^4 = 22$ ns. Using this time scale for the calculation of the dynamic moduli results in a too fast relaxation. As anticipated from theory in branched systems the process of arm retraction is suppressed exponentially with the arm length, thereby slowing down the full relaxation of the short arm. The short arm relaxation time following the calculation of Frischknecht for the asymmetric star is 0.8×10^{-5} s at room temperature which with the corresponding shift factor of $a_T = 5.71 \times 10^{-3}$ would correspond to about 46 ns at 509 K for PB. With the ratio of the entanglement time between PE and PB, the time scales are about a factor 1.4 larger for PE giving a relaxation time of about 64 ns. With this estimate and the used hopping fraction a hop diffusion constant of 0.21×10^{-7}cm^2/s would arise, implying a dynamics fast enough to be observed in the accessible NSE time range. Apparently, this is not the case. The time scale governing the short arm relaxation apparently is much longer (>190 ns) than expected. This finding is corroborated by the NSE result of a larger branch point friction which might slow down the relaxation even further.

B. Comparison with Simulation. Recently, Zhou and Larson[4] performed MD simulation on a similar branched polymer system. Following the trajectory of the branch point or center part of a corresponding linear chain, the localization of the star center has been shown, whereas in the case of the linear chain the diffusive motion of the chain center along the tube was revealed. For the case with our sample comparable asymmetric stars, the branch point was localized for times smaller than the short arm relaxation time, but for times longer than τ_s^*, the branch point displayed a distinctive hopping motion. This in time leads into a diffusive motion along the tube formed by the two long arms similar to the linear case. Following Zhou's argumentation, the time scales involved can be compared. The Rouse time of a non entangled chain with a fixed chain end is 4 times the Rouse time of a corresponding linear chain, which in our case of the short arm of the asymmetric star is about $\tau_s^R = 32$ ns. The actual time found in the simulation for the short arm to relax was about twice as much, which would give in our case $\tau_s^* \approx$ 70 ns. However, evidently, the star arm does not relax within the experimental time range of 190 ns. It seems that the short star arm is even more confined than anticipated from the simulation. Since the arm retraction time depends strongly on the number of entanglements of the short arm as $(N_s/N_e)^4$, for future experiments it should be possible to move the hopping motion into the NSE time domain by reducing the length of the short arm.

VI. Conclusion

With the combination of neutron spin echo spectroscopy and specific labeling of the branch point in a three-arm star the localization of the branch point has been shown for the first time directly on a molecular level. In comparison to a center labeled linear chain in the accessible time range the branch point is confined to a length scale somewhat smaller than the tube diameter for linear chains. A short arm of only one entanglement length leads to the same topological confinement of the branch point up to intermediate times. Only at longer times as accessed by rheology the asymmetric star displays a flow behavior similar to the linear chain. The dynamic modulus of the asymmetric star shows star-like features up to the terminal time of the linear chain. As was also reported in literature, the drag of the short arm is stronger than expected. This agrees with the NSE finding of a larger than expected friction of the branch point. In comparison to the MD simulation the experimental time scales are found to be even longer. Of course the comparison to rheology and simulation time scales might be affected by the differences in the investigated systems and different temperatures. However, all three techniques show that the restriction of the motion by a short side arm is stronger than expected. Probing the dependence of the arm length with NSE spectroscopy and accessing longer time scales might shed more light on the process of arm retraction.

References and Notes

(1) McLeish, T. C. B.; Milner, S. T. *Adv. Polym. Sci.* **1999**, *143*, 195.
(2) Milner, S. T.; McLeish, T. C. B. *Macromolecules* **1997**, *30*, 2159.
(3) Frischknecht, A.; Milner, S. T.; Pryke, A.; Young, R. N.; Hawkins, R.; McLeish, T. C. B. *Macromolecules* **2002**, *35*, 4801.
(4) Zhou, Q.; Larson, R. G. *Macromolecules* **2007**, *40*, 3443.
(5) Edwards, S. F. *Proc. Phys. Soc.* **1967**, *92*, 9.
(6) DeGennes, P. D. *J. Chem. Phys.* **1971**, *55*, 572.
(7) Likhtman, A. E.; McLeish, T. C. B. *Macromolecules* **2002**, *35*, 6332.
(8) Lee, J. H.; Fetters, L. J.; Archer, L. A. *Macromolecules* **2005**, *38*, 4484.
(9) Milner, S. T.; McLeish, T. C. B. *Macromolecules* **1998**, *31*, 7479.
(10) Rouse, P. E. *J. Chem. Phys.* **1953**, *21*, 1272.
(11) DeGennes, P. D. *J. Phys.* (*Paris*) **1981**, *42*, 735.
(12) Schleger, P.; Farago, B.; Lartigue, C.; Kollmar, A.; Richter, D. *Phys. Rev. Lett.* **1998**, *81*, 124.
(13) Doi, M.; Edwards, S. F. *The Theory of Polymer Dynamics*: Clarendon Press: Oxford, U.K., 1986.
(14) Wischnewski, A.; Monkenbusch, M.; Willner, L.; Richter, D.; Likhtman, A. E.; McLeish, T. C. B.; Farago, B. *Phys. Rev. Lett.* **2002**, *88*, 058301.
(15) Zamponi, M.; Wischnewski, A.; Monkenbusch, M.; Willner, L.; Richter, D.; Likhtman, A. E.; Kali, G.; Farago, B. *Phys. Rev. Lett.* **2006**, *96*, 238302.
(16) Zamponi, M.; Monkenbusch, M.; Willner, L.; Wischnewski, A.; Farago, B.; Richter, D. *Europhys. Lett.* **2005**, *72*, 1039.
(17) Vilgis, T. A.; Boué, F. J. *Polym. Sc.: Part B: Polym. Phys.* **1988**, *26*, 2291.
(18) Warner, M. *J. Phys. C: Solid State Phys.* **1981**, *14*, 4985.
(19) Mezei, F. *Neutron spin echo spectroscopy*; Lecture Notes in Physics 128; Springer: Berlin, 1980.
(20) Richter, D.; Farago, B.; Butera, R.; Fetters, L. J.; Huang, J. S.; Ewen, B. *Macromolecules* **1993**, *26*, 795.
(21) Fatkullin, N.; Kimmich, R. *Phys. Rev. E* **1995**, *52*, 3273.
(22) Fetters, L. J.; Lohse, D. J.; Colby, R. H. In *Physical Properties of Polymers handbook*; Mark, J. E., Ed.; Springer: Berlin, 2007; Chapter 25.
(23) Wischnewski, A.; Monkenbusch, M.; Willner, L.; Richter, D.; Kali, G. *Phys. Rev. Lett.* **2003**, *90*, 058302.
(24) Niedzwiedz, K.; Wischnewski, A.; Pyckhout-Hintzen, W.; Allgaier, J.; Richter, D.; Faraone, A. *Macromolecules* **2008**, *41*, 4866.